Navarra Center for International Development

Working Paper nº 04/2021

Detection of Trend Types in Surface Air Temperature in China

Xinxin Li

Chinese Academy of Sciences

Yan-Fang Sang

University of Chinese Academy of Sciences

Bellie Sivakumar

Indian Institute of Technology Bombay

Luis A. Gil-Alana

University of Navarra - Navarra Center for International Development

Navarra Center for International Development
WP-04/2021

Detection of Trend Types in Surface Air Temperature in China

Xinxin Li[1,2], Yan-Fang Sang[1*], Bellie Sivakumar[3], Luis A. Gil-Alana[4]

Abstract

Detection of trend types in temperature data, by distinguishing between deterministic and stochastic trends, has important implications for understanding climate change. The Unit root tests (URTs) have been widely used for detecting trend types, but they do not consider the possibility of fractional integration and its influences. In this study, we detected the trend types of surface air temperature observed during the period 1960–2019 at 558 stations across China, by considering fractional integration. The whole period was divided into three sub-periods by two structural breakpoints (denoted as SBP1 and SBP2). The fractional differencing parameter d was estimated by the Local Whittle (LW) function, and then the Phillips-Perron (PP), Kwiatkowski-Phillips-Schmidt-Shim, (KPSS) and Zivot and Andrews (ZA) tests were used to detect trend types in these temperature data. The results indicated that the de-seasoned monthly temperature (DMT) series are fractionally integrated and, thus, exhibit long-range dependence characteristics, which have significant influence on the estimation of trend slopes and detection of trend types. Compared with the LW function, the ordinary least squares yielded biased estimation of trend slopes, as it cannot handle the long-range dependence of DMT series, which generates pseudo trends and contaminates true trends of temperature. The DMT series with weak long-range dependence or anti-persistent characteristic were accurately detected as deterministic trends during 1960–SBP1, SBP1–SBP2, SBP2–2019. However, the DMT series with strong long-range dependence were detected as stochastic trend by KPSS test during SBP1–2019 and 1960–2019, which results from the oscillatory components from long-range dependence. Considering the fractional integration of time series and URTs together, therefore, is more appropriate to reliably detect trend types in temperature data. Following this, temperature over short periods in China were detected as having deterministic trends, but those at long periods were detected as having a combination of long-range dependence and deterministic trends.

Keywords: temperature variability; deterministic trend; stochastic trend; unit root test; fractional integration; long-range dependence

[1]Key Laboratory of Water Cycle and Related Land Surface Processes, Institute of Geographic Sciences and Natural Resources Research, Chinese Academy of Sciences, Beijing 100101, China, [2]University of Chinese Academy of Sciences, Beijing 101407, China, [3]Department of Civil Engineering, Indian Institute of Technology Bombay, Powai, Mumbai 400076, India, [4]University of Navarra, Pamplona, Spain.* Corresponding author: Tel/Fax: +86 10 6488 0471; E-mail: sangyf@igsnrr.ac.cn, sunsangyf@gmail.com

1. Introduction

Climate change is attracting much attention worldwide, due to its significant impacts on natural systems, human society, and economic development (Boo et al., 2004; Zhang et al., 2005; Zhang et al., 2009; Carrao et al., 2018; Duan et al., 2018; Zhang et al., 2018). As an important indicator of climate change, global temperature exhibits an increasing trend but also with significant variability (Qian and Qin, 2006; IPCC, 2014). Many studies have focused on how to accurately evaluate the significance of trend in temperature and its attribution (Liu et al., 2004; Qian and Lin, 2004; Li et al., 2013). The variability in temperature can be attributed to the greenhouse gases (GHGs), aerosols, and internal dynamics, such as the Atlantic Multidecadal Oscillation (AMO) and the Pacific Decadal Oscillation (PDO) (Wang et al., 2013; Chen and Tung, 2017; Gong et al., 2019). The linear trend, quantified by its slope, is a simple approach that is widely used to describe the temperature change at large timescales (Dai and Wang, 2010; Barbosa, 2011; Courtillot et al., 2013; Dittus et al., 2018). The estimation of linear trends is usually achieved by the ordinary least squares (OLS) method, which assumes that the residual (i.e., de-trended series) of time series is a random independent variable drawn from Gaussian distribution. However, such an assumption may not be satisfied by many temperature time series, whose residuals have dependent rather than independent characteristics (Gil-Alana and Sauci, 2019), thus causing a biased estimation of linear trends in temperature data.

The unit root process, denoted as difference stationarity, is an important representation of dependent characteristics of time series. A time series with unit root process has a stochastic trend rather than deterministic (including linear) trend, and two time series with unit root processes may present a spurious regression relationship (Kaufmann and Stern, 2002; Kaufmann et al., 2010). Thus, it is important to distinguish between deterministic and stochastic trends by considering unit root process, as a basis for obtaining accurate estimation of trends in temperature data.

The unit root tests (URTs) are widely used to detect unit root process and identify stochastic trends. There exist many different URTs, including the Dickey–Fuller (DF) test, augmented Dickey–Fuller (ADF) test, Phillips–Perron (PP) test, and the Kwiatkowski-Phillips-Schmidt-Shim (KPSS) test. The results from the different URTs, however, may often be different and inconsistent, and sometimes even contradictory, and lead to inaccurate interpretations and conclusions about the trend types. For example, regarding the global mean sea surface temperature (SST), the PP test suggests a deterministic trend, while the KPSS test suggests a stochastic trend (Barbosa, 2011). Some studies have reported that the contradictory results from the different URTs could be due to the presence of structural breaks (i.e., abrupt change-points) or shifts (i.e., turning points) in a time series, as they weaken and even invalidate the statistical tests (Gay-Garcia et al., 2009; Coggin, 2012) and cause biased KPSS test results. Besides, some other studies have suggested that noise in temperature data contaminates the signal of trend and further causes biased URT results. To overcome the influence of these factors, some studies have recently considered the cointegration relationship between the causative variables and the resulting variable, to detect unit root process and trend types in the latter. For example, the cointegration relationship between temperature (resulting variable) and radiative forcing (causative variable) was analyzed by Kaufmann and Stern (2002), Kaufmann et al. (2006a, b, 2010, 2011, 2013)). Since the radiative forcing was detected as a unit root process, temperature was suggested to have a stochastic trend in their studies, although its deterministic trend was directly detected by the PP test.

Regardless of whether the trend in temperature is directly detected by URTs or detected through the analysis of cointegration relationship, the analysis ignores the possibility of fractional integration, which is usually quantified by a fractional differencing parameter d and described as $I(d)$. Following the definition of fractional integration (Beenstock et al., 2012), a time series with deterministic trend is $I(0)$, unit root process is $I(1)$, and fractional integration is $I(d)$ ($0 < d < 1$). The PP and KPSS tests only assume that d is an integer equal to 1 and 0, respectively. Rejecting the null hypothesis of PP test means $d \neq 1$, but it cannot support $d = 0$; similarly, rejection of the null hypothesis of KPSS test means $d \neq 0$, but without supporting $d = 1$ (Beenstock et al., 2012). This implies that the PP and KPSS tests cannot give a definite testing result of deterministic or stochastic trend, because they do not consider the situations where $0 < d < 1$. Generally, the fractional differencing parameter d indicates the degree of long-range dependence in a time series, which means that the autocorrelation coefficient decays slowly following a power law and the next value in the time series requires knowledge of (often many) past values (Frich et al., 2002; Rybski et al., 2006, 2008). While the long-term correlations at large time-lags are individually small, their cumulative effects are non-negligible, and even may exhibit a visually significant trend in time series during sub-periods, although there is no sizeable trend over the whole period considered (Fatichi et al., 2009). There is increasing evidence showing that surface air temperature exhibits a long-range dependent behavior (Beran, 1994; Rybski et al., 2006; Franzke, 2012). Therefore, in view of the limitations of URTs and the possibility of inconsistent detection of trend in temperature (and other hydroclimatic) data, fractional integration should be considered for more reliable results.

Many studies have investigated the variability in temperature in China and its attribution (Zhai and Pan, 2003; Ren et al., 2005; Hua et al., 2008; Paranunzio et al., 2019; To and Yu, 2016; Hawkins and Sutton, 2009). However, the possible presence of a deterministic linear trend in temperature and its detection have not been properly addressed yet. The spatiotemporal variability in temperature and its complex underlying physical mechanisms make this problem particularly challenging. This provided the motivation for the present study. The main objective of this study was to detect the trend types of surface air temperature in China, by examining the influences of fractional integration. To be specific, the fractional differencing parameter (*d*) of the surface air temperature data at 558 stations across China during 1960–2019 were estimated by using the Local Whittle (LW) function; further, the results were compared with the results from the URTs to investigate the influence of long-range dependence on the detection of trend types by URTs.

The rest of this paper is organized as follows. Section 2 describes the data used in this study. Section 3 introduces the methods for estimating the fractional differencing parameter in temperature data and detecting trend types in temperature data, including the PP test, KPSS test, and Zivot and Andrews (ZA) test. Section 4 presents the results from the different methods, followed by a discussion in Section 5. Finally, conclusions are given in Section 6.

2. Data

The monthly surface air temperature data, measured at 558 meteorological stations across China, were used for this study. They have the same continuous period of 1960–2019. Considering that the variability in temperature at large timescale was of interest in this study, the de-seasoned monthly temperature (DMT) data (i.e., the average seasonal cycle was removed from the original data) were analyzed, to remove the influence of seasonal cycle on the results. To investigate the possible effects of structural breakpoints on the results of the URTs (see Section 3.2), the whole period 1960–2019 was divided into three sub-periods for comparison, with two breakpoints (denoted as SBP1 and SBP2) that were detected by the Zivot and Andrews (ZA) test (Zivot and Andrews, 1992). In each sub-period, the variability in temperature at long timescales tended to a monotonic trend. The periods of SBP1–2019 and 1960–2019 were also considered to understand the long-term variability in temperature, and the results for the periods of 1960–SBP1, SBP1–SBP2, SBP2–2019, SBP1–2019 and 1960–2019 were compared to examine the differences in the variability in temperature.

3. Methods

In this study, the fractional differencing parameter (d) of temperature data was assessed by the Local Whittle (LW) function (Gil-Alana and Sauci, 2019). The slope of linear trend in temperature data was also obtained from the LW function by considering long-range dependence. Further, the results were compared with those directly estimated by the ordinary least squares method, for investigating the influence of long-range dependence on the estimation of linear trends. The URTs (Fatichi et al., 2009), as conventional methods to distinguish deterministic trends from stochastic trends, were then used to detect trend types in temperature data, and they were compared with the fractional differencing parameters, to investigate the influence of long-range dependence on the detection of trend types by URTs.

3.1 Local Whittle function

The Local Whittle function is used to estimate the fractional differencing parameter *d* in fractional integration, which can be generally described as:

$$y_t = c + \beta t + x_t, \quad (1 - B)^d x_t = u_t, \quad t = 1, 2, ..., \tag{1}$$

where y_t is the time series to be analyzed, c is an intercept coefficient, β is the slope of a linear trend, *B* is the lag-operator (i.e., $Bx_t = x_{t-1}$), and u_t is a stationary noise component (i.e., $I(0)$) (Gil-Alana, 2015, 2016). The fractional differencing parameter *d* is estimated by the LW function in the frequency domain (Dahlhaus, 1989) along with a testing procedure from Robinson (1994), which tests the null hypothesis H_0:

$$H_0: \quad d = d_0, \tag{2}$$

which includes stationary ($d_0 < 0.5$) and non-stationary ($d_0 \geq 0.5$) characteristics. Generally, $d < 0$ means anti-persistent characteristics, while $d > 0$ displays a long-range dependence, and higher *d* reflects stronger long-range dependence (Gil-Alana, 2006, 2008).

3.2 Unit root test

The Dickey–Fuller (DF) test, augmented Dickey–Fuller (ADF) test, PP test, and KPSS test are widely used to detect unit root process and identify deterministic or stochastic trends of hydrometeorological data. Compared with the Dickey–Fuller test and the augmented Dickey–Fuller test (Dickey and Fuller, 1979; Said and Dickey, 1984), the PP and KPSS tests do not require stationary noise to be white noise data, thus allowing for serial correlation and heteroscedasticity, which is handled directly in the test statistic (Barbosa, 2011). Moreover, the null hypothesis of the PP test and the KPSS test are complementary, and their joint applications can yield more accurate results than a single test. To further consider the influences of structural breakpoints (SBPs) in a time series on the URTs results, the ZA test was also used to handle temperature data. The three methods are explained as follows.

(1) PP test. It has the null hypothesis of difference stationarity (i.e., stochastic trend) against the alternative of trend stationarity (i.e., deterministic trend) (Phillips, 1987). For a time series y_t, the PP test considers:

$$y_t = c + \beta t + a y_{t-1} + u_t. \tag{3}$$

The null hypothesis of difference stationarity is described by $a = 1$, against the alternative of $a < 1$. Rejection of the null hypothesis indicates that the trend of y_t (temperature series here) is deterministic.

(2) KPSS test. It has the null hypothesis of trend stationarity against the alternative of difference stationarity. The KPSS test considers:

$$y_t = c_t + \beta t + u_t, \tag{4}$$

where c_t is a random walk that presents a stochastic trend:

$$c_t = c_{t-1} + \varepsilon_t,\ \varepsilon_t \sim N(0, \sigma_\varepsilon^2). \tag{5}$$

If $\beta \neq 0 \Lambda \sigma_\varepsilon = 0$, then the model describes a trend stationary process and the variability in y_t can be characterized with a deterministic linear trend. When $\sigma_\varepsilon^2 \neq 0$, the model presents a difference stationary process, which indicates that the trend in the (temperature) time series is stochastic.

(3) ZA test. It has the advantages of allowing unknown structural breakpoints in a time series (Zivot and Andrews, 1992). It is based on the null hypothesis of difference stationarity (i.e., d = 1), which implies that the trend in the (temperature) series is stochastic, versus the alternative hypothesis of trend stationarity with a one-time break occurring at an unknown point. The ZA test considers three models:

$$y_t = c + \alpha y_{t-1} + \beta t + \gamma DU_t + u_t \tag{6.1}$$

$$y_t = c + \alpha y_{t-1} + \beta t + \theta DT_t + u_t \tag{6.2}$$

$$y_t = c + \alpha y_{t-1} + \beta t + \theta DU_t + \gamma DT_t + u_t, \tag{6.3}$$

where $\alpha = 1$ implies that the series y_t contains a unit root process, and $\alpha < 1$ implies that the series is a trend stationary process with a one-time break occurring at an unknown point. The term DU_t is a dummy variable for a mean shift occurring at each possible SBP, and DT_t is a corresponding trend shift variable. They are described as follows:

$$DU_t = \begin{cases} 1 \cdots\cdots if\, t > SBP \\ 0 \cdots\cdots otherwise \end{cases} \tag{7}$$

$$DT_t = \begin{cases} t - BP \cdots\cdots if\, t > SBP \\ 0 \cdots\cdots otherwise \end{cases} \tag{8}$$

The model in Equation (6.1) permits a one-time change in the average level of y_t, that in Equation (6.2) allows for a one-time change in the slope of the trend function, and that in Equation (6.3) combines one-time changes in the average level and the slope of the trend function of y_t. The ZA test was used to identify the main SBPs in each temperature data, based on which the whole period of 1960-2019 was divided into different sub-periods. In each sub-period, the trend type in temperature was detected by the PP, KPSS, and ZA tests together.

Figure 1 shows the flowchart for detection of deterministic or stochastic trends in the de-seasoned monthly temperature (DMT) series in China, by using the different approaches considered in this study.

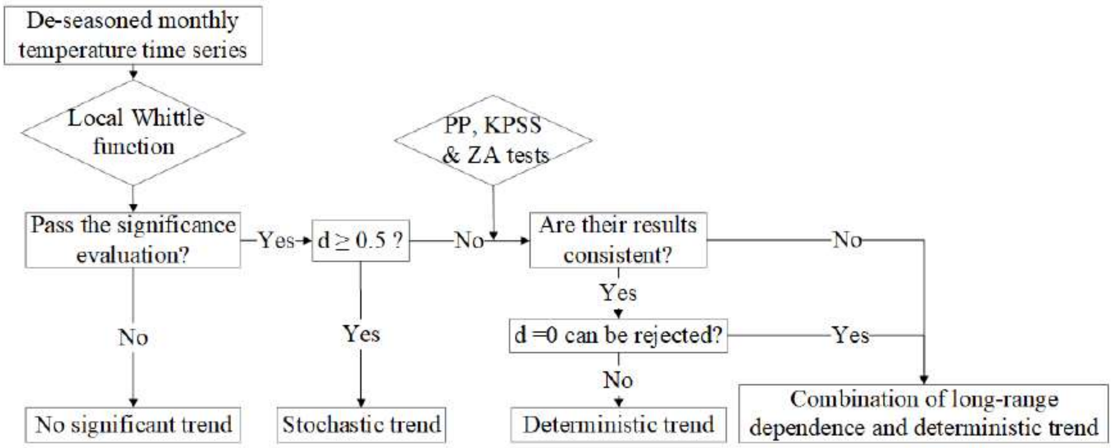

Figure 1. Flowchart for detection of deterministic or stochastic trends in de-seasoned monthly temperature (DMT) data in China. “PP test” is the Phillips-Perron test; “KPSS test” is the Kwiatkowski-Phillips-Schmidt-Shim test; “ZA test” is the Zivot and Andrews test; and “*d*” is the fractional differencing parameter.

4. Results

4.1. Estimation of fractional differencing parameter *d* in DMT data

The breakpoints of the 558 DMT series were identified by the ZA test. Figure 2 presents the results in the form of the frequency of break-time occurrence for all the 558 DMT series. The results indicated that the two main SBPs varied with the DMT series analyzed. The first structural breakpoint (SBP1) mainly occurred during 1970–1985, and the other (SBP2) occurred in 2000–2010. Each DMT series was divided into three parts using its two main breakpoints. Then, the fractional differencing parameter d of each DMT time series in 1960–SBP1, SBP1–SBP2, SBP2–2019, SBP1–2019, and 1960–2019 was estimated by the LW function. The results are presented in Figure 3 and Table 1. The results indicated that the d value was smaller than 0.5 for all DMT series during the five periods, implying that the DMT series were fractionally integrated and their trends were not stochastic (i.e., deterministic). During 1960–SBP1, the 389 DMT series with $d < 0$ exhibited anti-persistent characteristic in China, except the stations in the north of the Songliao River basin and upper reaches of the Yellow and Yangtze River basins, where DMT data exhibited long-range dependence. The 316 DMT series in the Yangtze River basin during SBP1–SBP2, and 305 DMT series in the Yellow and Yangtze River basins during SBP2–2019, had $d < 0$, versus d value of 0~0.5 in the other regions, implying that these DMT series exhibited long-range dependence. During SBP1–2019 and 1960–2019, as many as 444 DMT series (except those in the lower reaches of the Yangtze River basin) and 539 DMT series, respectively, had much bigger d values than those in the former three sub-periods, indicating the stronger long-range dependence of DMT series over the longer periods. The 95% confidence level of d values was further estimated (Table 1). The results indicated that the 464, 470, 430, 425, and 131 DMT series failed to reject $d = 0$ at 95% confidence level in the five sub-periods, respectively.

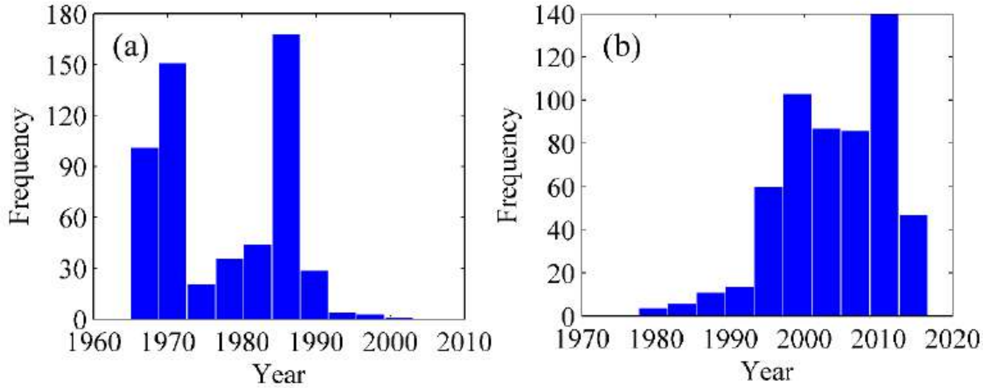

Figure 2. Frequency of break-time occurrence of structral breaks (denoted as SBP1 and SBP2) in the de-seasoned monthly temperature (DMT) data at 558 stations in China: (a) SBP1, and (b) SBP2.

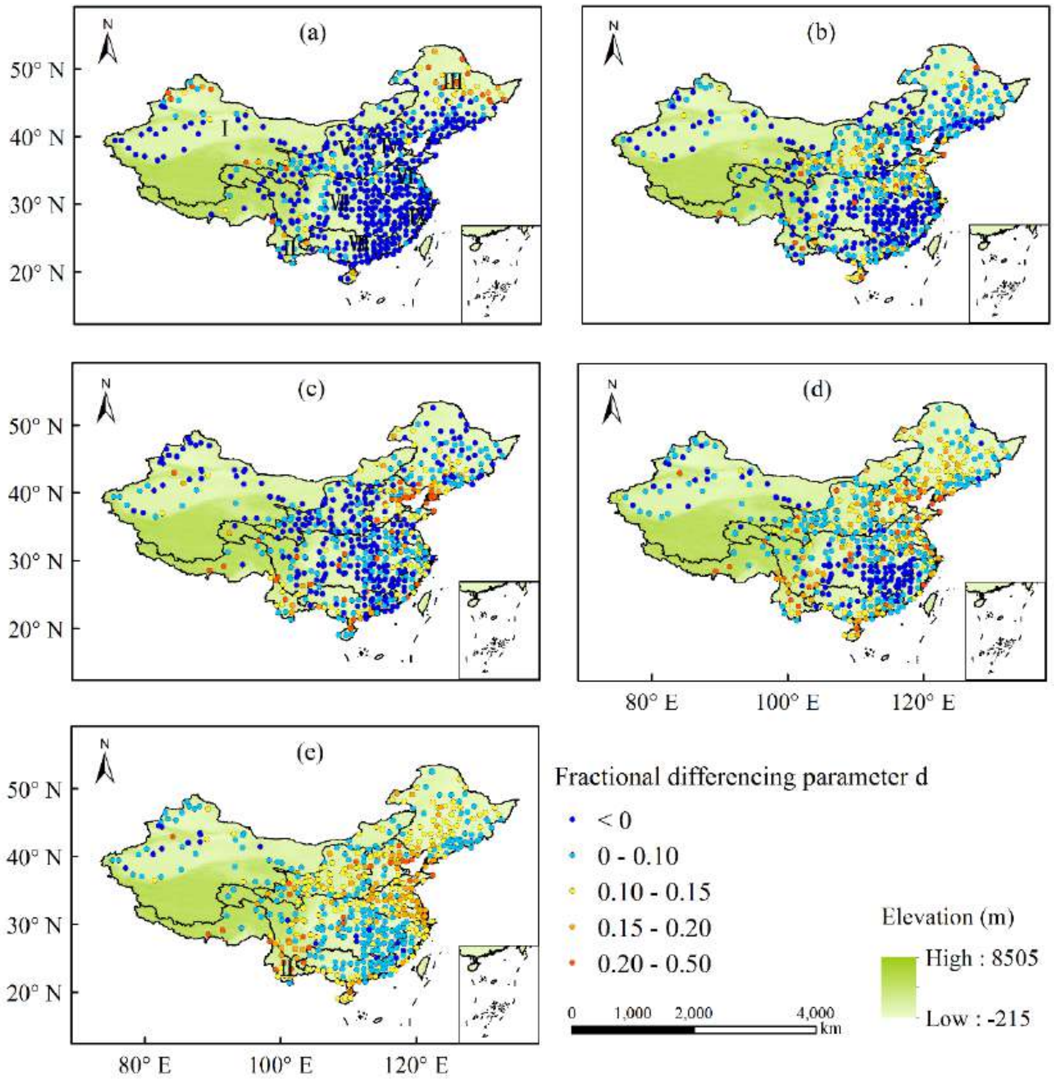

Figure 3. Fractional differencing parameter *d* in the de-seasoned monthly temperature (DMT) data at 558 stations in China using the Local Whittle function: (a) 1960–SBP1, (b) SBP1–SBP2, (c) SBP2–2019, (d) SBP1–2019, and (e) 1960–2019. The grey stations mean the insignificant trends of DMT data. I: Inland River Basin; II: Southwest River Basin; III: Songliao River Basin; IV: Hai River Basin; V: Yellow River Basin; VI: Huai River Basin; VII: Yangtze River Basin; VIII: Pearl River Basin; IX: Southeast Rivers Basin.

<Insert Table 1>

The above results suggest that the DMT series were fractionally integrated and exhibited much stronger long-range dependence during SBP1–2019 and 1960–2019 than that during 1960–SBP1, SBP1–SBP2, and SBP2–2019. This implies that the DMT series cannot be simply detected as a single deterministic trend or stochastic trend and, therefore, that the URTs should be cautiously used for the detection of the trend types in DMT series by considering fractional integration.

4.2 Influence of long-range dependence on trend slope of DMT

The estimated slopes of linear trends in the DMT series by the LW function, considering the influence of long-range dependence, are displayed in Figure 4 and Table 2. During the period 1960–SBP1 (Fig. 4(a)), only 47 DMT series exhibited significant upward trends. During SBP1–SBP2 (Fig. 4(b)), however, as many as 482 DMT series (distributed almost all over China) showed significant upward trends, with a notable exception of the stations in Southwest China. Ren et al. (2005) drew a similar conclusion that the temperature warming in China had mainly occurred since the last two decades of the 20th century, which was perhaps due to the high emission of GHGs. During SBP2–2019 (Fig. 4(c)), significant linear trends of 305 DMT series were mainly observed in the Huai, Hai, Yellow and Yangtze River basins. This is in agreement with the observations reported by some recent studies that global mean surface temperature has been exhibiting a smaller warming rate since 2000 (Trenberth and Fasullo, 2014; Yan et al., 2016). During SBP1–2019 (Fig. 4(d)) and 1960–2019 (Fig. 4(e)), nearly all the DMT series (512 and 531, respectively) showed significant trends, with higher significance level in North China.

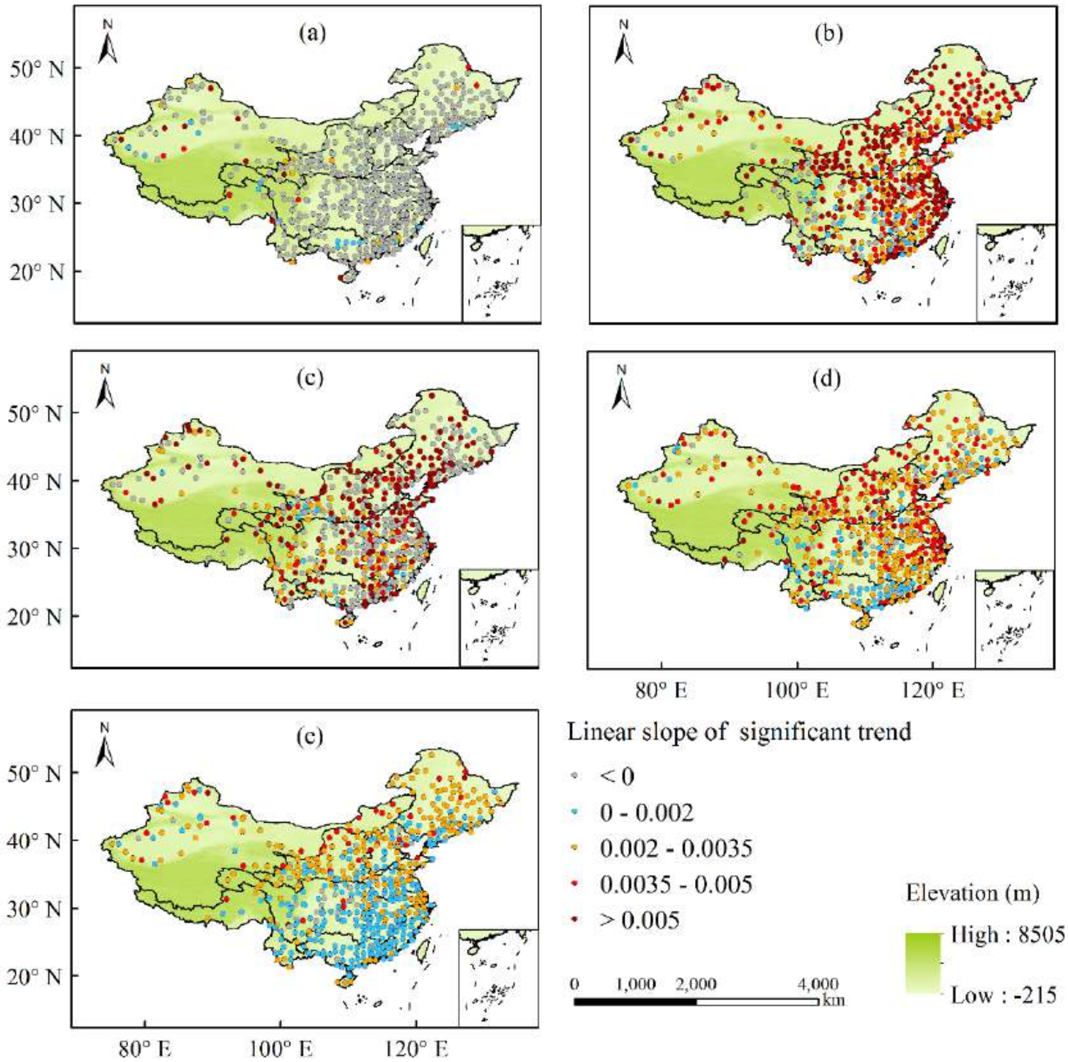

Figure 4. Spatial distribution of the trend slopes by the Local Whittle function in the de-seasoned monthly temperature (DMT) data at 558 stations in China: (a) 1960–SBP1, (b) SBP1–SBP2, (c) SBP2–2019, (d) SBP1–2019, and (e) 1960–2019.

<Insert Table 2>

To investigate the influence of long-range dependence on the slopes of linear trends in the DMT series, the trends were also estimated by the OLS method and then compared with the above results using the LW function. Note that the significance of the linear trend was not considered here, for the convenience of comparison. The results in Figures 5 and 6 show that the trend slopes in the DMT series estimated by the two methods are different. During 1960–SBP1, the slopes of the downward trends estimated by the OLS method were larger than that by the LW function for 403 DMT series, indicating that the OLS method would overestimate the trend slopes, because it does not consider the long-range dependence of the DMT series. To be specific, the long-range dependence of the DMT series during 1960–SBP1 indicated pseudo-downward trends, which were overlapped with the true downward trends and caused the overestimation of the OLS method. However, for the DMT series in Southwest China and the boundary of the Yellow and Yangtze River basins, the trend slopes were underestimated by the OLS method due to the pseudo-upward trends from the long-range dependence of the DMT data over there. Similarly, for the DMT series in the south part of the Yangtze River basin and some other regions during SBP1–SBP2, in East China during SBP2–2019, in south of the Yangtze River basin during SBP1–2019, and all over China during 1960–2019, their trend slopes were overestimated by the OLS method. In such cases, the long-range dependence exhibited pseudo-upward trends, which overlapped with the actual upward trend and further caused the overestimation of the upward trend in the DMT series by the OLS method. These different results between the LW function and the OLS method imply the necessity of considering long-range dependence to identify linear trends in the DMT series.

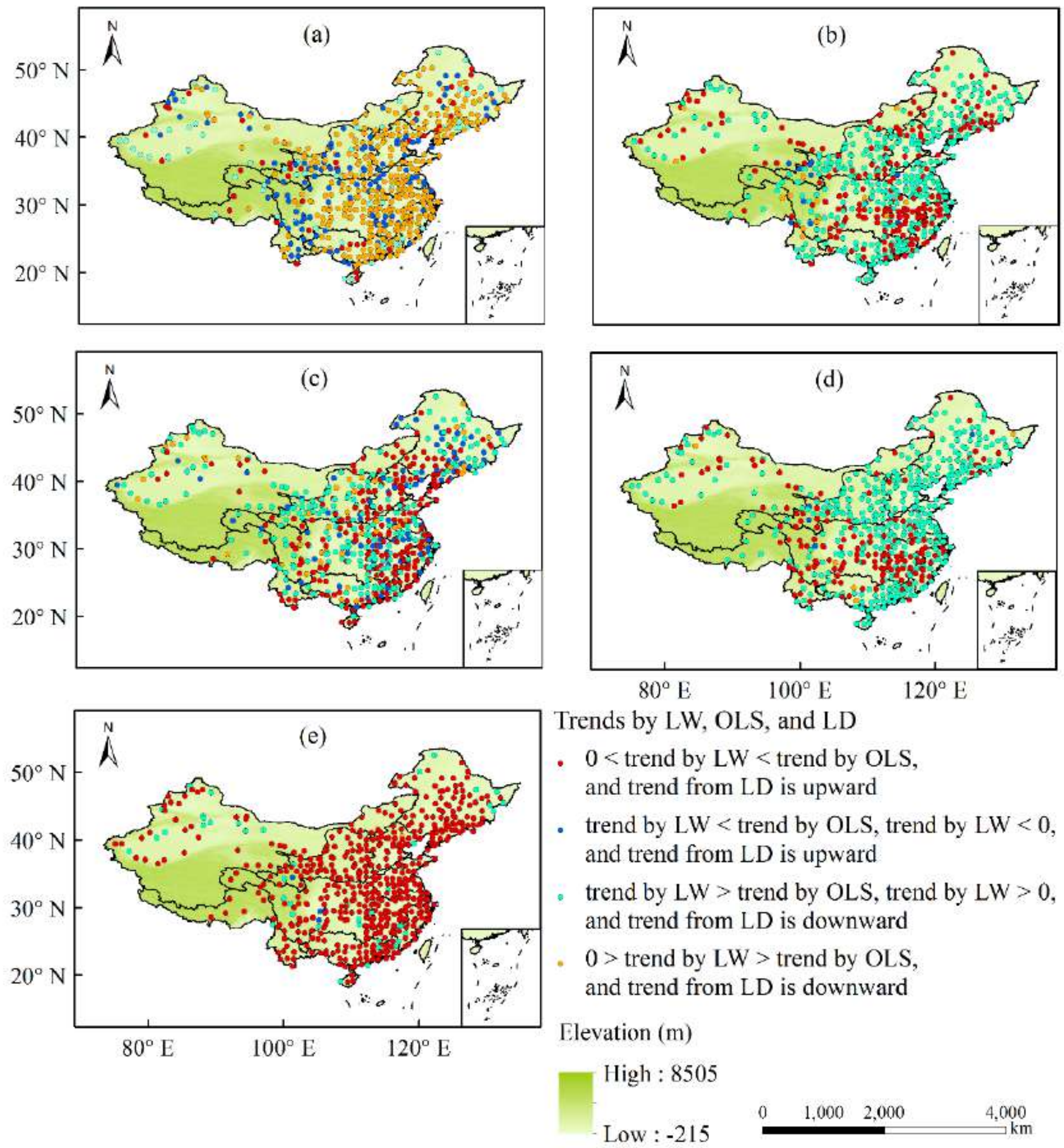

Figure 5. Trend slopes by the Local Whittle function (LW), ordinary least squares (OLS), and LD (long-range dependence) in the de-seasoned monthly temperature (DMT) data at 558 stations in China: (a) 1960–SBP1, (b) SBP1–SBP2, (c) SBP2–2019, (d) SBP1–2019, and (e) 1960–2019.

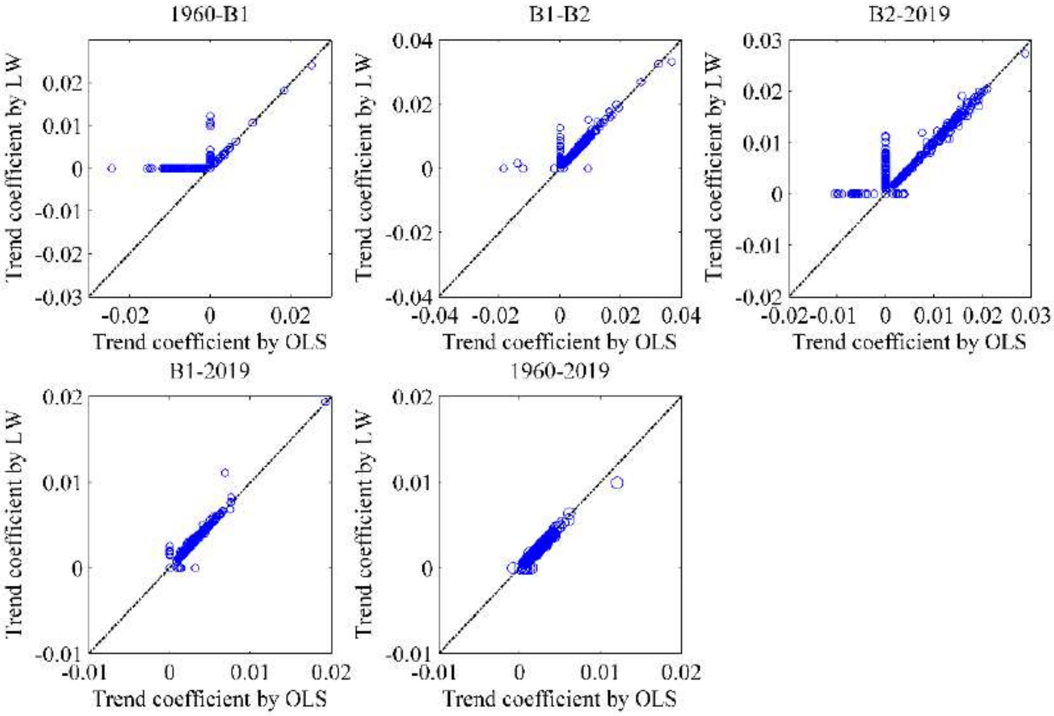

Figure 6. Changes in trend slopes in the de-seasoned monthly temperature (DMT) data by ordinary least squares (OLS) and the Local Whittle (LW) function during 1960–SBP1, SBP1–SBP2, SBP2–2019, SBP1–2019, and 1960–2019. Here, the DMT data measured at 558 stations in China are considered.

4.3 Influence of long-range dependence on trend types by unit root tests

The PP, KPSS, and ZA tests were applied to distinguish deterministic trends from stochastic trends in the 558 DMT series, and the results are presented in Table 2. The results show that the PP and ZA tests rejected the null hypothesis of difference stationarity (stochastic trend) at all the 558 stations, while the KPSS test rejected the null hypothesis of trend stationarity (deterministic trend) at 13, 81, 97, 241, and 427 stations during 1960–SBP1, SBP1–SBP2, SBP2–2019, SBP1–2019, and 1960–2019, respectively.

To investigate the influence of long-range dependence on the detection of trend types by the URTs, the fractional differencing parameter d value of the DMT series was further compared with the results of the URTs for the five periods. The DMT series with $d = 0$ were detected to reject the null hypothesis of difference stationarity (stochastic trend) by the PP and ZA tests (results not shown here), implying that their trends tend to be deterministic rather than stochastic. The results of the KPSS test are shown in Table 3 and Figure 7, where the DMT series exhibited stronger long-range dependence characteristics during SBP1–2019 and 1960–2019 than that during 1961–SBP1, SBP1–SBP2, and SBP2–2019. The DMT series (459, 430, 393, 228, and 48 in the five sub-periods) with $d = 0$ at 95% confidence level were detected as deterministic trends by the KPSS test, and the DMT series (8, 41, 60, 202 and 377) with $d \neq 0$ were detected as stochastic trends. The results indicated that the DMT series with stronger long-range dependence were more likely to be detected as stochastic trends by the KPSS test during SBP1–2019 and 1960–2019, while the trends in the DMT series with $d = 0$ during 1961–SBP1, SBP1–SBP2, and SBP2–2019 were generally detected as deterministic by the KPSS test.

<Insert Table 3>

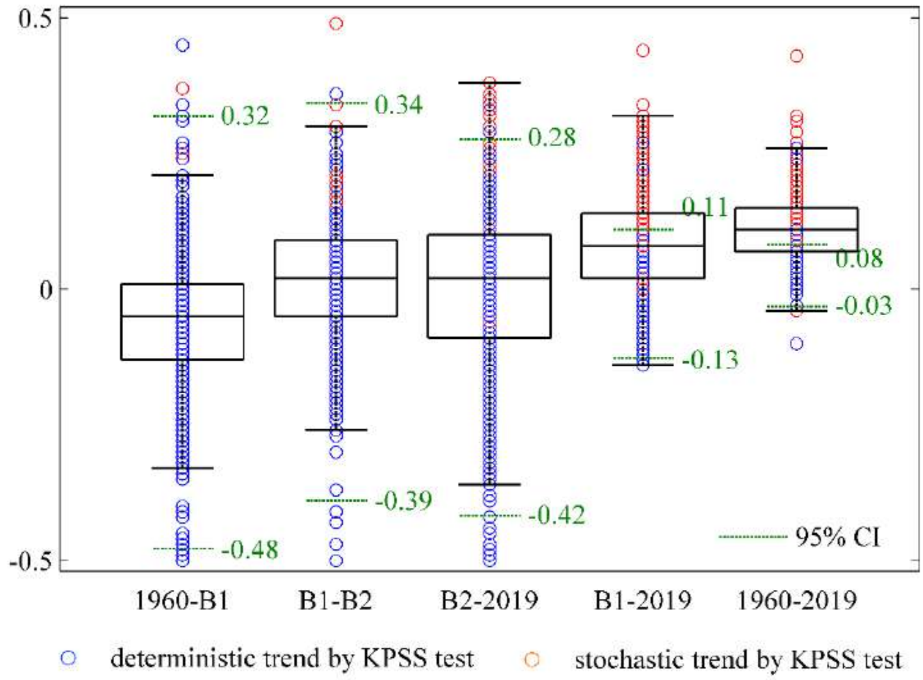

Figure 7. Fractional differencing parameter *d* and its boxplot in the de-seasoned monthly temperature (DMT) data at 558 stations in China, and the 95% confidence interval (CI) of $d = 0$ during 1960–SBP1, SBP1–SBP2, SBP2–2019, SBP1–2019, and 1960–2019.

The above results suggest that the performances of URTs were significantly influenced by the long-range dependence in the DMT data. Generally, the temperature variability consists of linear deterministic component, stationary noise, and oscillatory components resulting from long-range dependence. The former two components can be detected as trend stationary or stationary by the URTs, and thus would not influence the detection of trend types by the URTs. However, the oscillatory components from long-range dependence would be wrongly detected as stochastic trend by the KPSS test. Moreover, stronger long-range dependence would generate more significant oscillatory components in the DMT series during a longer period, leading to false detection of trend types in the DMT series by the KPSS test.

During 1960–SBP1, SBP1–SBP2, and SBP2–2019, the DMT series with anti-persistent characteristic (i.e., $d < 0$) or weak long-range dependence (i.e., $0 < d$ and $d = 0$ cannot be rejected at 95% confidence level) exhibited weak oscillatory components, whose influence on the results from the KPSS test can be ignored and, thus, they were rightly detected as deterministic trend by the KPSS test. For the DMT series during SBP1–2019 and 1960–2019, the oscillatory components from strong long-range dependence become much more significant (i.e., $0 < d$ and $d = 0$ can be rejected at 95% confidence level), which had big influence on the detection of trend types by the KPSS test and caused the wrong detection of stochastic trends in the DMT series. Furthermore, the oscillatory components cannot be described with a unit root process ($d = 1$) and, thus, the null hypothesis of stochastic trend in the PP and ZA tests were rejected for all the DMT series.

4.4 Determination of trend types in DMT series

It is important to recognize that one cannot expect to always obtain fractional differencing parameter $d = 0$ for hydroclimate data, even when there is no or weak long-range dependence in hydroclimate data. Thus, the fractional differencing parameter d and the URTs were used together here to determine the trend types in the DMT series, by considering significance level of trends together. To be more specific, if the fractional differencing parameter $d > 0.5$, then the significant linear trend in the corresponding DMT series was regarded as stochastic. If the fractional differencing parameter d = 0 cannot be rejected and the results of all PP, KPSS, and ZA tests indicated trend stationarity (difference stationarity), then the significant linear trend in the corresponding DMT series was regarded as deterministic. Otherwise, the variability of temperature was considered to be a combination of long-range dependence and deterministic trend. However, the insignificant linear trends were not considered here for the detection of URTs.

Table 2 and Figure 8 present the results of trend types in the DMT data. The significant linear trends were detected as deterministic in 23 DMT series during 1960–SBP1, in 366 DMT series during SBP1–SBP2 (except some regions in the Yangtze and Yellow River basins), and in 228 DMT series during SBP2–2019 (in some regions of the Yangtze, Yellow, and Songliao River basin). Besides, the trends of dozens of DMT series were detected as a combination of long-range dependence and deterministic trend during the above three periods. During SBP1–2019, the significant deterministic trends of 218 DMT series were observed in the Yangtze River basins, whereas the trend of 294 DMT series were detected as the combinations of long-range dependence and deterministic trend. During 1960–2019, as many as 485 DMT series were identified to be combinations of long-range dependence and deterministic trend, but the significant linear trends in 46 DMT series (in the Songliao and Inland River basins) were detected as deterministic.

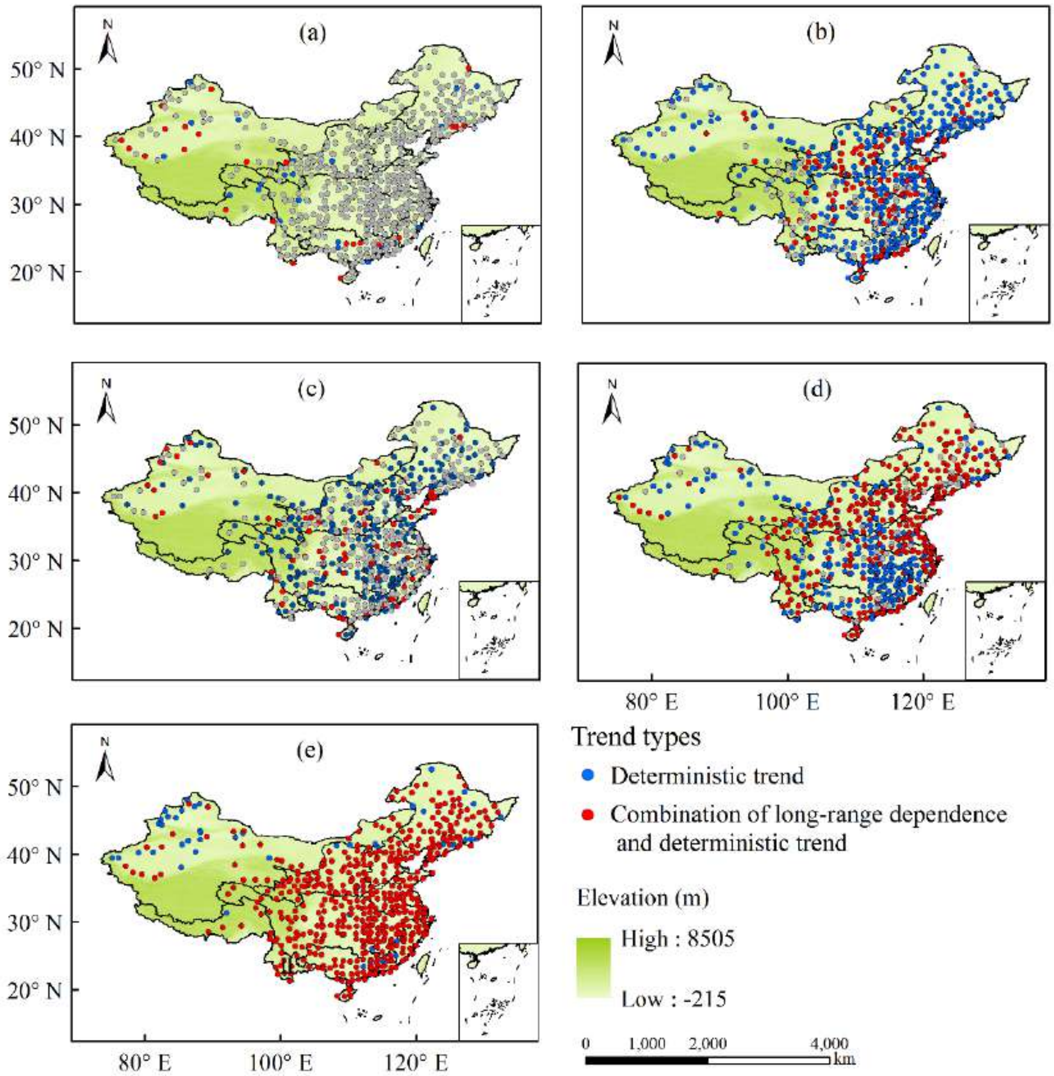

Figure 8. Trend types of the de-seasoned monthly temperature (DMT) data at 558 stations in China using the PP, KPSS, and ZA tests: (a) 1960–SBP1, (b) SBP1–SBP2, (c) SBP2–2019, (d) SBP1–2019, and (e) 1960–2019. "PP test" is the Phillips-Perron test; "KPSS test" is the Kwiatkowski-Phillips-Schmidt-Shim test; "ZA test" is the Zivot and Andrews test.

5. Discussion

The above results suggested that the long-rage dependence has great influence on the detection of trend types in DMT data. While previous studies have reported that the structural breakpoints in a time series would also cause biased (and even false) detection of trend types by URTs. Their relationship is tried to clarify here. The trends in the DMT series without breakpoints during 1961–SBP1, SBP1–SBP2, and SBP2–2019 were basically detected as deterministic. Comparatively, the DMT series with two (one) structural breakpoints during 1960–2019 (SBP1–2019) tended to be detected as stochastic trends by the KPSS test. The results here seemly support the influence of structural breakpoints in a time series. However, it should be noticed that the long-range dependence characteristics would generate natural oscillations, which inevitably include structural breakpoints in a time series, especially for long time series. Therefore, it is more reasonable to take long-range dependence as the essential cause that influence the performance of different URTs, and further influence the detection of trend types in temperature data.

Besides, some studies (e.g., Werner et al., 2015) have used segment trends (i.e., step changes) to describe the variability in temperature, because the variability in temperature can be better described with segmented trends than a simple linear trend. The different climate components have different intrinsic timescales and quasi-oscillatory climate models and, thus, climate systems at global and regional scales have been changing in complex ways (Keenlyside et al., 2008; Knight et al., 2009; Franzke, 2010; Sang et al., 2018). This well explains the appearance of segmented trends over sub-periods to describe the variability in temperature. In fact, the non-monotonic variability in temperature consists of deterministic component (resulting from external forcing) and oscillatory components (resulting from natural forcing) (Xu et al., 2015), which exhibit short-range and long-range dependence characteristics. The deterministic component generally can be described with segmented trends and well interpreted by external forcing, but the oscillatory components caused by natural forcing cannot be explained well with segmented trends in terms of physical mechanisms. Especially, there is increasing evidence showing that surface air temperature exhibits a long-range dependent behavior (Beran, 1994; Franzke, 2012). Therefore, it is not appropriate to simply use segmented trends while dealing with temperature data and describing its long-term variability.

6. Conclusions

Detection of the variability in temperature is important to understand the changes in climate and its potential impacts. In climate change-related studies, the linear trend is frequently used for describing the long-term variability in temperature. This practice assumes that the residual (i.e., de-trended series) of the time series is a random independent variable drawn from Gaussian distribution. However, residual of temperature data usually has dependent, rather than independent, characteristics, which further influences the detection of the significance of linear trends and trend types (deterministic or stochastic). In this study, we considered the possibility of fractional integration that is used widely to describe the dependent characteristics of time series and investigated whether the trend in surface air temperature in China is deterministic or stochastic.

The fractional differencing parameter d of 558 de-seasoned monthly temperature (DMT) series over China was estimated by the Local Whittle (LW) function. Considering the possible effects of structural breakpoints on the results of the URTs, the whole period 1960–2019 was divided into three sub-periods with two breakpoints (denoted as SBP1 and SBP2). The results suggested that the DMT series were fractionally integrated and that they exhibited much stronger long-range dependence during SBP1–2019 and 1960–2019 than that during 1960–SBP1, SBP1–SBP2 and SBP2–2019. The trends estimated by the LW function were compared with that by the OLS method. The results indicated that the OLS method gave biased results of trend slopes in temperature data, because it cannot handle the pseudo trends generated from the long-range dependence of series.

Furthermore, the results of the PP, KPSS, and ZA tests were compared with the fractional differencing parameter *d*, and the influences of long-range dependence on the detection of trend types by the URTs were investigated. The results showed that the DMT series with weak long-range dependence or anti-persistent characteristic were accurately detected as deterministic trends during 1960–SBP1, SBP1–SBP2, and SBP2–2019. However, the DMT series with strong long-range dependence were detected as stochastic trend by the KPSS test during SBP1–2019 and 1960–2019, which resulted from the oscillation components from long-range dependence. The URTs and the fractional differencing parameter *d* were considered together to better detect the trend types of the DMT series in China, and the results reflect that temperature in China over short periods have a deterministic trend but have a combination of long-range dependence and deterministic trend during long periods.

In summary, it would not be appropriate to directly use OLS and URTs (such as the PP and KPSS tests) to detect the trend types in temperature and evaluate their significance level, as these methods do not consider the possibility of fractional integration of time series and their influences on the detection of trend types and significance of linear trend. Considering the fractional integration of time series and various URTs together is a more proper approach to detecting trend types in temperature data. However, to further understand the variability of temperature in China, the complex physical mechanisms still need to be studied, by considering the effects of internal climate dynamics and other external forcing factors.

Acknowledgments

The temperature data were obtained from the National Meteorological Information Center of China Meteorological Administration (CMA) (http://data.cma.cn/). This study was financially supported by the National Key Research and Development Program (No. 2019YFA0606903), the National Natural Science Foundation of China (No. 41971040), the Youth Innovation Promotion Association of CAS (No. 2017074), and the CAS Interdisciplinary Innovation Team (No. JCTD-2019-04).

References

Barbosa, S.M., 2011. Testing for deterministic trends in global sea surface temperature. J. Clim. 24, 2516–2522.

Beenstock, M., Reingewertz, Y., Paldor, N., 2012. Polynomial cointegration tests of anthropogenic impact on global warming. Earth Syst. Dyn. 3(2), 173–188.

Beran, J., 1994. Statistics for Long Memory Processes. CRC Press, London, England.

Boo, K.O., Kwon, W.T., Kim, J.K., 2004. Vegetation change in the regional surface climate over East Asia due to global warming using BIOME4. Il. Nuovo. Cimento. C. 27, 317–327.Carrao, H., Naumann, G., Barbosa P., 2018. Global projections of drought hazard in a warming climate: a prime for disaster risk management. Clim. Dyn. 50(5–6), 2137–2155.

Chen, X.Y., Tung, K.K., 2017. Global-mean surface temperature variability: space-time perspective from rotated EOFs. Clim. Dyn. 51, 1719–1732.

Coggin, T.D., 2012. Using econometric methods to test for trends in the HadCRUT3 global and hemispheric data. Int. J. Climatol. 32, 315–320.

Courtillot, V., Mouel, J.L.L., Kossobokov, V., Gibert, D., Lopes, F., 2013. Multi-decadal trends of global surface temperature: a broken line with alternating ~30 yr linear segments?. Atmos. Clim. Sci. 3, 364–371.

Dahlhaus, R., 1989. Efficient parameter estimation for self-similar process. Ann. Stat. 17, 1749–1766.

Dai, X.G., Wang, P., 2010. Zonal mean mode of global warming over the past 50 years. Atmos. Oceanic Sci. Lett. 3, 45–50.

Dickey, D.A., Fuller, W.A., 1979. Distributions of the estimators for autoregressive time series with a unit root. J. Am. Stat. Assoc. 74(366), 427–481.

Dittus, A.J., Karoly, D.J., Donat, M.G., Lewis, S.C., Alexander, L.V., 2018. Understanding the role of sea surface temperature-forcing for variability in global temperature and precipitation extremes. Weather. Clim. Extremes 21, 1–9.

Duan, Y.W., Wu, P.L., Chen, X.L., Ma, Z.G., 2018. Assessing global warming induced changes in summer rainfall variability over Eastern China using the latest Hadley Centre Climate Model HadGEM3-GC2. Adv. Atmos. Sci. 35, 1077–1093.

Fatichi, S., Barbosa, S.M., Caporali, E., Silva, M.E., 2009. Deterministic versus stochastic trends: Detection and challenges. J. Geophys. Res.-Atmos. 114: D18121.

Franzke, C., 2010. Long-range dependence and climate noise characteristics of Antarctic temperature data. J. Clim. 23(22), 6074–6081.

Franzke, C., 2012. Nonlinear trends, long-range dependence, and climate noise properties of surface temperature. J. Clim. 25, 4172–4183.

Frich, P., Alexander, L.V., Della-Marta, P.M., Gleason, B., Haylock, M., Tank, A.K., Peterson, T., 2002. Observed coherent changes in climatic extremes during the second half of the twentieth century. Clim. Res. 19, 193–212.

Gay-Garcia, C., Estrada, F., Sánchez, A., 2009. Global and hemispheric temperatures revisited. Clim. Change 94, 333–349.

Gil-Alana, L.A., 2006. Nonstationarity, long memory and anti-persistence in several climatological time series. Environ. Model. Assess. 11(1), 19–29.

Gil-Alana, L.A., 2008. Time trend estimation with breaks in temperature time series. Clim. Change. 89(3–4), 325–337.

Gil-Alana, L.A., 2015. Linear and segmented trends in sea surface temperature data. J. Appl. Stat. 42(7), 1531–1546.

Gil-Alana, L.A., 2016. Alternative modelling approaches for the ENSO time series. Persistence and seasonality. Int. J. Climatol. 37(5), 2354–2363.

Gil-Alana, L.A., Sauci, L., 2019. US temperatures: Time trends and persistence. Int. J.

Climatol. 39(13), 5091–5103.
Gong, H., Wang, L., Chen, W., Wu, R., 2019. Time-varying contribution of internal dynamics to wintertime land temperature trends over the Northern Hemisphere. Geophys. Res. Lett. 46, 1–10.
Hawkins, E., Sutton, R., 2009. The potential to narrow uncertainty in regional climate predictions. Bull. Amer. Meteor. Soc. 90, 333–337.
Hua, L.J., Ma, Z.G., Guo, W.D., 2008. The impact of urbanization on air temperature across China. Theor. Appl. Climatol. 93, 179–194.
IPCC, 2014. Climate Change 2014: Synthesis Report. Contribution of Working Groups I, II and III to the fifth Assessment Report of the Intergovernmental Panel on Climate Change. [Core Writing Team, Pachauri, R.K., Meyer, L.A (eds.)]. Geneva, Switzerland.
Kaufmann R.K., Stern, D.I., 2002. Cointegration analysis of hemispheric temperature relations. J. Geophys. Res. 107, D2.
Kaufmann, R.K., Kauppi, H., Stock, J.H., 2006a. Emissions, concentrations and temperature: a time series analysis. Clim. Change. 77, 249–278
Kaufmann, R.K., Kauppi, H., Stock. J.H., 2006b. The relationship between radiative forcing and temperature: what do statistical analyses of the instrumental temperature record measure? Clim. Change. 77, 279–289
Kaufmann, R.K., Kauppi, H., Stock, J.H., 2010. Does temperature contain a stochastic trend? Evaluating conflicting statistical results. Clim. Change. 101, 395–405.
Kaufmann, R.K., Kauppi, H., Mann, M.L., Stock, J.H., 2011. Reconciling anthropogenic climate change with observed temperature 1998–2008. Proc. Natl. Acad. Sci. 108(29), 11790–11793.
Kaufmann, R.K., Kauppi, H., Mann, M.L., Stock, J.H., 2013. Does temperature contain a stochastic trend: linking statistical results to physical mechanisms. Clim. Change. 118, 729–743.
Keenlyside, N.S., Latif, M., Jungclaus, J., Kornblueh, L., Roeckner, E., 2008. Advancing decadal-scale climate prediction in the North Atlantic sector. Nature 453, 84–88.
Knight, J., Kennedy, J.J., Folland, C.K., Harris, G., Jones, G.S., Palmer, M., Parker, D., Scaife, A., Stott, P., 2009. Do global temperature trends over the last decade falsify climate predictions? State of the Climate in 2008. Bull. Amer. Meteor. Soc. 90, S22–S24.
Li, J.F., Zhang, Q., Chen, Y.D., Singh, V.P., 2013. GCMs-based spatiotemporal evolution of climate extremes during the 21st century in China. J. Geophys. Res.-Atmos. 118, 1–19.
Liu, B.H., Xu, M., Henderson, M., Qi, Y., Li, Y.Q., 2004. Taking China's temperature: daily range, warming trends, and regional variations, 1955–2000. J. Clim. 17,

4453–4462.

Paranunzio, R., Ceola, S., Laio, F., Montanari, A., 2019. Evaluating the effects of urbanization evolution on air temperature trends using nightlight satellite data. Atmosphere, 10, 117.

Phillips, P.C.B., 1987. Time series regression with a unit root. Econometrica 55, 277–301.

Qian, W.H., Lin, X., 2004. Regional trends in recent temperature indices in China. Clim. Res. 27, 119–134.

Qian, W.H., Qin, A., 2006. Spatial-temporal characteristics of temperature variation in China. Meteorol. Atmos. Phys. 93, 1–16.

Ren, G.Y., Chu, Z.Y., Zhou, Y.Q., Xu, M.Z., Wang, Y., 2005. Recent progresses in studies of regional temperature changes in China. Clim. Environ. Res. 10, 701–717 (in Chinese with English abstract).

Robinson, P.M., 1994. Efficient tests of nonstationary hypotheses. J. Am. Stat. Assoc. 89, 1420–1437.

Rybski, D., Bunde, A., Havlin, S., von Storch, H., 2006. Long-term persistence in climate and the detection problem. Geophys. Res. Lett. 33(6), L06718.

Rybski, D., Bunde, A., Havlin, S., von Storch, H., 2008. Long-term memory in 1000-year simulated temperature records, J. Geophys. Res. 113, D02106

Said, S.E., Dickey, D.A., 1984. Testing for unit roots in autoregressive-moving average models of unknown order. Biometrika 71, 599–607.

Sang, Y.F., Sun, F.B., Singh, V.P., Xie, P., Sun, J., 2018. A discrete wavelet spectrum approach for identifying non-monotonic trends in hydroclimate data. Hydrol. Earth Syst. Sci. 22, 755–766.

Trenberth, K.E., Fasullo, J.T., 2014. An apparent hiatus in global warming?. Earth's Future 1, 19–32.

To, W.M., Yu, T.W., 2016. Characterizing the urban temperature trend using seasonal unit root analysis: Hong Kong from 1970 to 2015. Adv. Atmos. Sci. 33, 1376–1385.

Wang, J.L., Yang, B., Ljungqvist, F.C., 2013. The relationship between the Atlantic Multidecadal Oscillation and temperature variability in China during the last millennium. J. Quat. Sci. 28, 653–658.

Werner, R., Valev, D., Danov, D., Guineva, V., 2015. Study of structural break points in global and hemispheric temperature series by piecewise regression. Adv. Space Res. 56, 2323–2334.

Xu, Y., Gao, X.J., Shi, Y., Zhou, B.T., 2015. Detection and attribution analysis of annual mean temperature changes in China. Clim. Res. 63, 61–71.

Yan, X.H., Boyer, T., Trenberth, K., Karl, T.R., Xie, S.P., Nieves, V., Tung, K.K., Roemmich, D., 2016. The global warming hiatus: Slowdown or redistribution?. Earth's Future 4, 1–11.

Zivot, E., Andrews, D.W. K., 1992. Further Evidence on the Great Crash, the Oil-Price Shock, and the Unit-Root Hypothesis. J. Bus. Econ. Stat. 10(3), s251–270.

Zhai, P.M., Pan, X.H., 2003. Trends in temperature extremes during 1951–1999 in China. Geophys. Res. Lett. 30, 169–172.

Zhang, D., Jim, C.Y., Lin, C.S., He, Y.Q., Lee, F., 2005. Climate change, social unrest and dynastic transition in ancient China. Chinese Sci. Bull. 50, 137–144.

Zhang, J., Chen, H., Zhang, Q., 2018. Extreme drought in the recent two decades in northern China resulting from Eurasian warming. Clim. Dyn. 6, 1–18.

Zhang, Q., Xu, C.Y., Zhang, Z.X., Chen, Y.D., 2009. Changes of temperature extremes for 1960–2004 in Far-West China. Stoch. Environ. Res. Risk Assess. 23, 721–735.

Table 1. Results of the fractional differencing parameter d for the de-seasoned monthly temperature data measured at 558 stations in China.

Period	$d < 0$	$0 < d < 0.5$	$d = 0$ at 95% confidence level	$d \neq 0$ at 95% confidence level
1960–SBP1	389	169	464	94
SBP1–SBP2	242	316	470	88
SBP2–2019	253	305	430	128
SBP1–2019	114	444	425	133
1960–2019	19	539	131	427

Table 2. Results of the significance evaluation of linear trends, unit root tests, and trend types for the de-seasoned monthly
temperature data measured at 558 stations in China.

Period	Significant linear trend	Trend stationarity			Difference stationarity			Trend type		
		PP test	KPSS test	ZA test	PP test	KPSS test	ZA test	Deterministic	Stochastic	Combination of long-range dependence and deterministic trend
1960–SBP1	47	558	545	558	0	13	0	23	0	24
SBP1–SBP2	482	558	477	558	0	81	0	366	0	116
SBP2–2019	305	558	461	558	0	97	0	228	0	77
SBP1–2019	512	558	317	558	0	241	0	218	0	294
1960–2019	531	558	131	558	0	427	0	46	0	485

Table 3. Detection of trend types by the KPSS test for the de-seasoned monthly temperature data measured at 558 stations in China.

Period	1960–SBP1		SBP1–SBP2		SBP2–2019		SBP1–2019		1960–2019	
	Trend stationary	Difference stationary	Trend stationary	Difference stationary	Trend stationary	Difference stationary	Trend stationary	Difference stationary	Trend stationary	Difference stationary
$d = 0$ at 95% confidence level	459	5	430	40	393	37	228	39	48	50
$d \neq 0$ at 95% confidence level	86	8	47	41	68	60	89	202	83	377